Vibrational Spectroscopy xxx (2017) xxx-xxx

Contents lists available at ScienceDirect

Vibrational Spectroscopy

journal homepage: www.elsevier.com

Infrared spectroscopic studies on crystalline phase transition of PVDF and PVDF/hyperbranched polyester blend ultrathin films

D. Manjula Dhevi[a], A. Anand Prabu[b,*], Kap Jin Kim[c,**]

[a] Department of Chemistry, Faculty of Science & Humanities, SRM University, Kattankulathur, Kanchipuram District, Tamil Nadu 603203, India
[b] Department of Chemistry, School of Advanced Sciences, VIT University, Vellore, Tamil Nadu 632014, India
[c] Department of Advanced Materials Engineering for Information and Electronics, College of Engineering, Kyung Hee University, Gyeonggi-do 446-701, Republic of Korea

ARTICLE INFO

Article history:
Received 10 July 2017
Received in revised form 22 November 2017
Accepted 8 December 2017
Available online xxx

Keywords:
Polyvinylidene fluoride
Hyperbranched polyester
Heat treatment
FTIR spectroscopy
Factor analysis
Crystalline phase

ABSTRACT

In this study, as cast (AC, at 30 °C) and annealed (AN, at 130 °C, 3 h) samples of polyvinylidene fluoride (PVDF) and PVDF/hyperbranched polyester (HBP) (90/10) blend ultrathin films were subjected to heating-cooling (30→210→30 °C) cycle, and studied for their changes in crystalline phase transition behavior using in situ Fourier transform infrared-transmission spectroscopy (FTIR-TS) and grazing incident reflection absorption spectroscopy (FTIR-GIRAS) techniques. Factor analysis was employed to extract the pure crystalline and amorphous spectra as well as the percentage content of ferroelectric crystallinity for both the samples. Irrespective of the thermal treatment (AC or AN) and spectral measurement (FTIR-TS or GIRAS) techniques, neat PVDF sample exhibited irreversible phase transitions during heating-cooling cycle associated with the transformation from ordered β-crystalline (1276 cm^{-1}) into disordered amorphous (1234 cm^{-1}) form. Interestingly, annealed PVDF/HBP blend sample measured using FTIR-GIRAS exhibited reversible crystalline phase transition behavior similar to a 'dipole memory effect' even after heating to 210 °C (>T_m) and then cooled to 30 °C. Compared to neat PVDF, higher ferroelectric crystallinity and reversible phase transition in PVDF/HBP blend may be attributed to (i) the existence of H-bonding between HBP (C═O and OH groups) and PVDF (–CH_2 and –CF_2) and/or (ii) HBP acting as a nanoparticle in PVDF matrix.

1. Introduction

In recent times, organic electronics, especially polymeric thin film based memories have generated much interest among researchers and technologists due to their ease of preparation, flexibility, miniaturized dimensions, low-cost potential, low voltage operation, large capacity for data storage, mechanical stability, etc. [1–6]. Among many materials, ferroelectric polymers such as vinylidene fluoride-trifluoroethylene [P(VDF-TrFE)] copolymers with VDF content 50–85 mol% have gained attraction for use in non-volatile random access memory (NvRAM) devices due to their large spontaneous polarization of about 0.1 C/m^2 [7,8], excellent polarization stability [9,10], switching times as short as 0.1 μs [11], better chemical stability [12] and low-temperature sample processing conditions [13]. Though many researchers have favored P(VDF-TrFE) due to its aforementioned advantages [7–13], it is imperative to focus our attention on improving the ferroelectric characteristics of polyvinylidene fluoride (PVDF) homopolymer which exhibits polarization only under stretching or poling of its thick films [14,15], due to its cheaper raw material cost and presence of higher C-F dipoles in the main chain compared to P(VDF-TrFE).

Formation of polar β-crystalline form in PVDF thick films can be increased by the addition of hydrated salts [15], ionic liquids (IL) [16–18], nanoparticles [19–21], clay [22,23], nanotubes [24–26], etc. Zhu et al. reported an increase in longer all-*trans* (β-crystalline) sequence formation with increasing IL loading in PVDF. Compared to slow-cooling from melt, the higher formation of polar β- and γ-crystalline forms in melt-quenched PVDF is attributed to the ion-dipole interactions between IL and PVDF chains [18]. On the other hand, PVDF nanoscale films prepared using spin-casting technique exhibit an interesting crystalline phase transition behavior compared to its thick film case. In our recent studies, ferroelectric β-crystalline content calculated using FTIR spectral data in spin-cast (at 30 °C) PVDF ultrathin films [27] was found to be higher (~71%) compared to that of P(VDF-TrFE) (~47%) case [28]. Also, a smaller addition (10 wt.%) of hyperbranched polyester (HBP) significantly increased the β-crystalline phase content in PVDF by 23% which is attributed to the H-bonding between carbonyl and/or hydroxyl groups of HBP and –CH_2 or –CF_2 of PVDF [27]. Hence, instead of increasing the β-crystalline form in PVDF thick films under the influence of varying additives or under mechanical deformation, the β-crystalline form in PVDF can be easily increased by preparing spin-cast films of nanoscale thickness or by blending with HBPs as discussed above.

Until now, very few researchers have studied the phase transition behavior in ferroelectric polymers under a heating-cooling cycle. Yang et al. reported a significant reduction in the overall crystallinity and ferroelectricity in P(VDF-TrFE-chlorofluoroethylene) terpolymer

* Corresponding author.
** Corresponding author.
Email addresses: anandprabu@vit.ac.in (A. Anand Prabu); kjkim@khu.ac.kr (K.J. Kim)

https://doi.org/10.1016/j.vibspec.2017.12.003
0924-2031/

with increasing temperature during the heating cycle [29]. From FTIR-GIRAS data, during heating (above melting, T_m)-cooling cycle, an irreversible phase transition between the polar (ferroelectric) and non-polar (paraelectric) crystalline phase at T_c was observed [30]. Our research group has also reported the structural phase transition in spin-cast P(VDF-TrFE) ultrathin films as a function of varying FTIR measurement modes [28], film thickness [31] and heating–cooling temperature range [30]. Also, Factor Analysis (FA) of the FTIR data was effectively used to extract the pure crystalline and amorphous phase spectra as well as to determine the quantitative changes in β-crystalline content during the heating-cooling cycle [28,31].

Interestingly, no previous reports are available in the literature pertaining to FTIR phase transition studies of PVDF and PVDF/HBP blend during heating-cooling cycle. In continuation of our earlier published works on PVDF [15,20] and PVDF/HBP [27], our objectives in the present study are to analyze the crystalline phase transition behavior in spin-cast PVDF and PVDF/HBP (90/10, in wt.%) blend ultrathin film samples measured using two different FTIR spectroscopic modes, viz. (a) FTIR-transmission spectroscopy (TS) and (b) FTIR-grazing incident reflection absorption spectroscopy (GIRAS) modes as a function of two different sample preparation conditions (as-cast at 30 °C (AC); annealed at 130 °C (AN)) during a heating-cooling (30→210 ($>T_m$)→30 °C) cycle.

2. Experimental

2.1. Materials

PVDF (M_w = 60,000) powder was received from Polysciences Inc. (U.S.A.). KBr disks (for FTIR-TS measurement), acetone and DMF were purchased from Sigma–Aldrich (U.S.A.) and used as received. ITO coated glass substrates (for FTIR-GIRAS measurement) purchased from SD Tech. (Korea) were cleaned using a 3-step process, viz. immersing in soap solution, acetone-deionized water (1:1, v/v) mixture and isopropanol-deionized water (1:1, v/v) mixture in a series of 2 h each. The ITO substrates were further dried under nitrogen gun, kept in a vacuum oven at 100 °C for overnight and stored in desiccator for further use.

2.2. Sample preparation

Synthesis and characterization of third generation HBP (based on pentaerythritol as a core molecule and dimethylol propionic acid as AB_2 monomer) [32], and its miscibility and crystallization behavior with PVDF were reported in our previous studies [27]. In the present study, calculated amount of PVDF and its blend with HBP (90/10, w/w) were dissolved in filtered acetone: DMF (80:20, v/v) mixture to form a 2 wt.% solution and kept stirring at 50 °C in a water bath for overnight. The filtered homogenous and transparent solutions of PVDF and PVDF/HBP (90/10) were spin-cast (1500 rpm for 30 s; step speed 500 rpm) at 30 °C on KBr and ITO substrates using a heat-controlled spin coating (HCSC) set-up (refer to Fig. 2 in Ref. [33]). Thermal annealing of the spin-coated samples was carried out at 130 °C, 3 h in vacuo followed by slow-cooling to room temperature. As-cast (at 30 °C) and annealed (at 130 °C, < T_m) ultrathin films prepared in this study are henceforth referred to 'AC' and 'AN' samples, respectively, and subjected to a heating-cooling (30→210→30 °C) cycle.

2.3. Characterization techniques

Unpolarized FTIR-TS and FTIR-GIRAS (at an incident angle of ca. 85 °C from normal to the surface) spectra were recorded using Bruker 66 V FTIR spectrophotometer at a resolution of 2 cm^{-1}. After mounting the sample in a custom-made heating cell, FTIR spectra were recorded as follows: heating from 30 to 210 °C (ramp, 1 °C/min), soak at 210 °C for 10 min (to remove the thermal history) and cooling from 210 to 30 °C (ramp, −1 °C/min). The raw spectra were smoothened (15°) by Savitsky-Golay method, base-line corrected, normalized and used for further analysis.

3. Results and discussion

3.1. Phase transition studies using FTIR-TS

Fig. 1 represents the FTIR-TS spectra recorded during heating–cooling (30→210→30 °C) cycle for both AC and AN samples of (a) PVDF and (b) PVDF/HBP (90/10) blend as a function of varying phase transition temperatures. During heating cycle (30→210 °C), both AC-PVDF and AC-blend samples undergo crystalline phase transition from low-temperature to high-temperature phase. The A_1 (1276 cm^{-1}) band assigned to ferroelectric crystalline phase and sensitive to sequences of four or more *trans* form (C–F) is decreased sharply in absorption intensity during heating cycle. The absorption intensity of B_1 band at 1405 cm^{-1} assigned to chain (C–C) orientation does not change considerably even when the sample transformed to

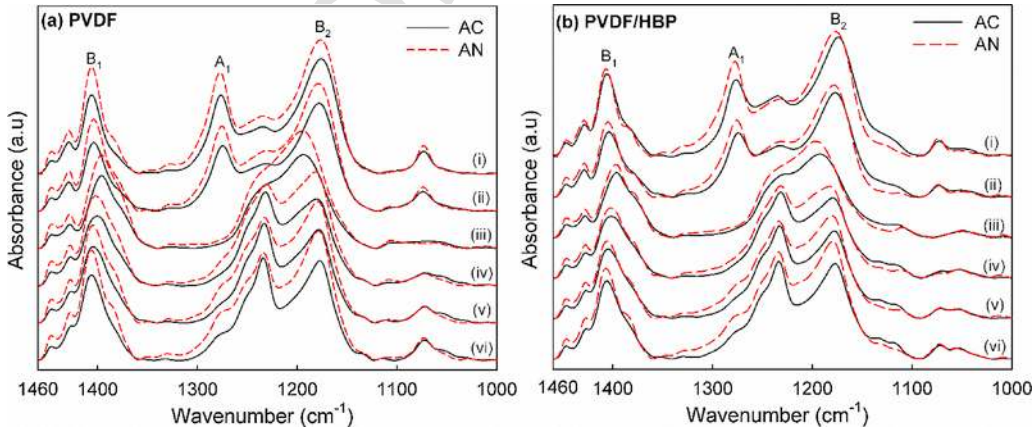

Fig. 1. FTIR-TS: Temperature induced changes in (a) PVDF and (b) PVDF/HBP (90/10) samples (AC and AN) as a function of heating(H)–cooling(C) sequence in the order of (i) 30H, (ii) 140H, (iii) 210H, (iv) 140C, (v) 80C and (vi) 30C.

high-temperature phase, since the *trans-gauche* conformational change is considered to occur without any changes in the chain orientation direction as reported by Tashiro et al. [34,35]. During the cooling cycle (210→30 °C), the all-*trans* form associated with A_1 band is converted into the disordered amorphous phase (1234 cm^{-1}) which is an evidence for the irreversible *β*-crystalline phase transition upon cooling from melt. Phase transition behavior in AN-PVDF and AN-blend samples were observed to be similar to that of AC samples though with higher A_1 band intensity, and is attributed to the enhanced ferroelectric *β*-crystalline content aided by the partial conversion of disordered polymer chains existing in AC condition into more ordered *β*-crystalline form in AN samples.

In order to confirm the suitability of the materials for the fabrication of NvRAM devices, it is imperative to not only control their crystalline structure but also to identify the application of thermal range in which the samples exhibit their ferroelectric characteristics. A clear change in the crystalline content is not easily identified from the qualitative spectral analysis as shown in Fig. 1, and hence, we focused our attention on studying the quantitative changes in crystalline (A_1) sensitive bands using FA of the spectral data obtained from heating-cooling studies. From raw FTIR data analysis, it is very difficult to identify non-overlapping bands of crystalline and amorphous-phase bands due to the fact that the raw IR data is a mixture spectra of both the phases existing together. Hence, it becomes even more difficult to extract the pure spectrum of each phase and to calculate their content in each sample. Our research group has effectively used FA to identify the number of independent components in the mixture spectra and the concentration of each pure component present in the mixture [27,28,31,36]. The theoretical aspects of FA have already been published in our earlier report [28]. 358 data points were taken into consideration in the frequency range of 1460–1000 cm^{-1} for all the samples used in the present study.

3.1.1. FTIR-TS: factor analysis of AC samples

The spectral features of the low-temperature ($<T_m$) and high-temperature ($>T_m$) phases extracted using FA of PVDF-AC (27 spectra) and blend-AC (23 spectra) samples during heating-cooling (30→210→30 °C) cycle are discussed in this section. From Table 1 of FA data, the $(IND)_k$ function between the first maxima and the minima show the presence of 8 and 6 components in the mixture spectra for PVDF-AC and blend-AC, respectively. The initial assumption was that each sample from heating–cooling studies exists with the major component present being either the low- or high-temperature crystalline phase. The other following components (from 3rd) may be factors related to the changes in the chain orientation, surface scattering, etc. and their magnitude is assumed to be negligible or much less when compared to the changes in the low- or high-temperature phase contents. As shown in Table 1, the first and the second eigenvalues and their corresponding eigenspectra were employed by FA to extract the product spectrum of PVDF and its blend samples (Fig. S1 in *Supplementary Information*). The minima and maxima at 1275 and 1231 cm^{-1}, respectively of the product spectrum were employed for obtaining the pure-component spectra. The extracted pure low-temperature (crystalline) and high-temperature (amorphous) phase spectra as shown in Fig. 2 are designated as PuS-1 and PuS-2, respectively. Narrow and well-defined PuS-1 peaks at

Table 1
FTIR-TS: FA data of PVDF and PVDF/HBP (90/10) AC and AN samples subjected to heating-cooling (30→210→30 °C) cycle.

Components	PVDF-AC		PVDF/HBP-AC		PVDF-AN		PVDF/HBP-AN	
	Eigenvalue	IND × 10^4	Eigenvalue	IND × 10^4	Eigenvalue	IND × 10^4	Eigenvalue	IND × 10^4
1.	25.02510	**0.1669**	21.40430	**0.2018**	24.14730	**0.1732**	24.09280	**0.1783**
2.	0.799000	**0.0785**	0.476700	**0.1019**	0.750300	**0.0667**	0.795300	**0.0696**
3.	0.167200	**0.0194**	0.109400	**0.0329**	0.094200	**0.0211**	0.100000	**0.0253**
4.	0.005758	**0.0127**	0.006751	**0.0205**	0.006036	**0.0122**	0.007801	**0.0166**
5.	0.002114	**0.0077**	0.002283	**0.0105**	0.000891	**0.0105**	0.002092	**0.0131**
6.	0.000206	**0.0077**	0.000145	**0.0105**	0.000558	**0.0090**	0.000541	**0.0127**
7.	0.000167	**0.0076**	0.000109	0.0106	0.000212	**0.0087**	0.000323	0.0128
8.	0.000138	**0.0074**	0.000065	0.0112	0.000113	0.0088	0.000244	0.0131
9.	0.000077	0.0076	0.000063	0.0116	0.000071	0.0093	0.000130	0.0140
10–20	Not shown here							
21.	0.000010	0.0340	0.000005	0.2247	0.000009	0.0531	0.000028	0.0881
22.	0.000007	0.0472	0.000004	0.7554	0.000009	0.0780	0.000025	0.1300
23.	0.000007	0.0700	0.000002	–	0.000008	0.1285	0.000022	0.2134
24.	0.000006	0.1175			0.000006	0.2650	0.000018	0.4382
25.	0.000005	0.2551			0.000004	1.0047	0.000013	1.5517
26.	0.000004	0.9506			0.000004	–	0.000009	–
27.	0.000003	–						

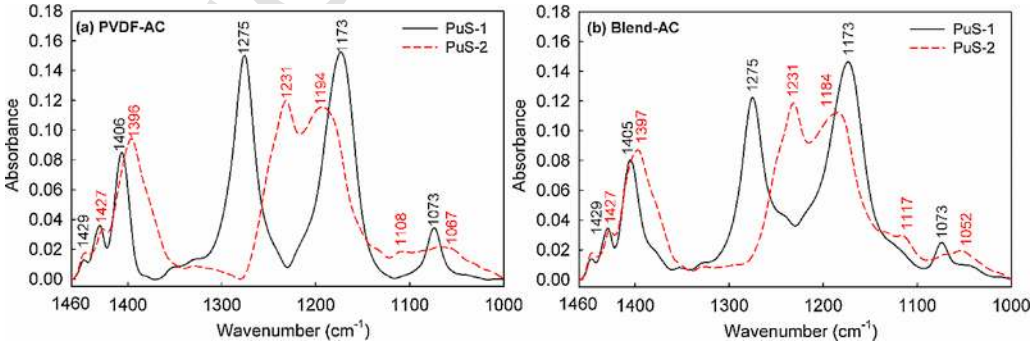

Fig. 2. FTIR-TS: Extracted pure-component spectra (PuS-1 and 2) using FA of (a) PVDF and (b) PVDF/HBP blend (90/10). As-cast (AC) samples were used in this study.

1275, 1173 and 1073 cm^{-1} for both the samples are assigned to the ferroelectric pure β-crystalline phase which is predominant at lower temperature of the heating-cooling cycle. 1173 and 1073 cm^{-1} bands do partially overlap with PuS-2 bands (amorphous phase) at 1194, 1067 cm^{-1} for PVDF and 1184, 1052 cm^{-1} for blend samples and hence not considered as pure crystalline spectral bands. Interestingly, the band appearing at 1275 cm^{-1} for both the samples is non-overlapping with any of the amorphous phase bands and hence used for measuring crystalline content. Likewise, the 1231 cm^{-1} band in PuS-2 for both the samples is identified as the non-overlapping amorphous phase band in addition to the non-overlapping amorphous phase bands at 1108 (PVDF) and 1117 cm^{-1} (blend).

Fig. 3 exhibits the percentage content of all-*trans* β-crystalline phase quantitatively calculated using FA of the FTIR-TS data measured during heating-cooling cycle. The β-crystalline content at 30 °C for both PVDF-AC and blend-AC were calculated as 59% and 67%, respectively, during the heating cycle. When the same samples were cooled to 30 °C from melt (at 210 °C), the β-crystalline content drastically reduced to 27% and 25%, respectively. The amount of crystalline content observed after cooling to 30 °C is almost equivalent to the crystalline content at near 190 °C during heating cycle for both the samples. Both the samples exhibit melting behavior at near 180 °C, which may result in the loss of polarization through an ordered (crystalline) → disordered (amorphous) phase transition and the formation of a statistical combination of TG, TG′, T_3G and T_3G' isomers packed in a disordered lattice during this phase transition [31,37–39].

3.1.2. FTIR-TS: factor analysis of AN samples

Table 1 shows the FA data carried out using 26 spectra each of PVDF-AN and blend-AN samples selected from the heating-cooling cycle. Based on $(IND)_k$ function between the first maxima and minima, 7 and 6 components could be present in PVDF-AN and blend-AN, respectively. Corresponding abstract eigenspectra based on those components and product spectra obtained from the first and second abstract eigenspectra are shown in Fig. S2. The minima and maxima at 1225 and 1276 cm^{-1} for PVDF-AN, and the minima and maxima at 1231 and 1276 cm^{-1} for blend-AN were chosen for obtaining the pure component spectra. The extracted pure crystalline (PuS-1) and amorphous (PuS-2) phase spectra for both the samples are shown in Fig. 4. PuS-1 of both the samples exhibits well-defined crystalline bands at 1276, 1173 (1175 cm^{-1} for blend-AN) and 1073 cm^{-1}. Though the bands at 1173 and 1073 cm^{-1} partially overlap with the high-temperature (PuS-2) phase bands, the peak appearing at 1276 cm^{-1} is non-overlapping with any of the PuS-2 bands and hence considered for measuring the pure ferroelectric phase crystalline content for both the samples. Interestingly, the 1231 cm^{-1} peak identified as the non-overlapping band in AC condition overlaps with PuS-1 peaks in the AN condition, and hence, non-overlapping bands at 1106 cm^{-1} (PVDF-AN) and 1110 cm^{-1} (blend-AN) in PuS-2 were treated as pure amorphous phase bands.

Fig. 5 presents the quantitative changes in ferroelectric β-crystalline phase content of PVDF-AN and blend-AN samples during heating-cooling cycle. The amount of β-crystalline content in PVDF-

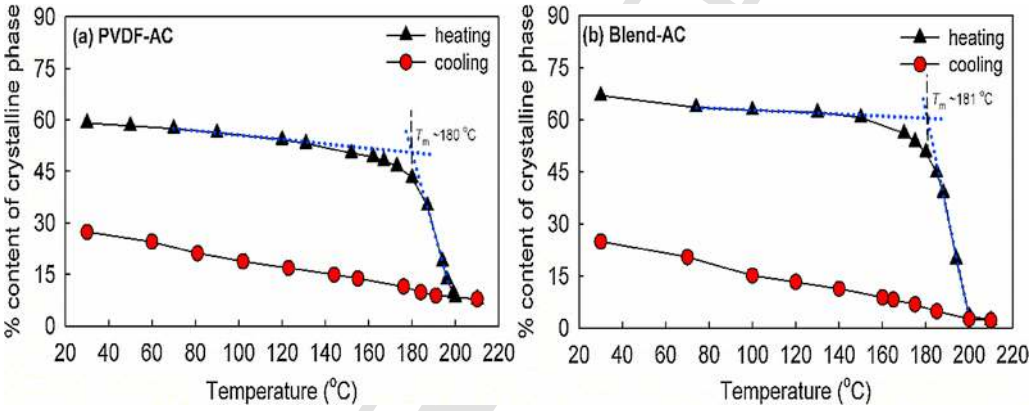

Fig. 3. FTIR-TS: Percentage content of β-crystalline phase calculated using FA of (a) PVDF and (b) PVDF/HBP blend (90/10). As-cast (AC) samples were used in this study.

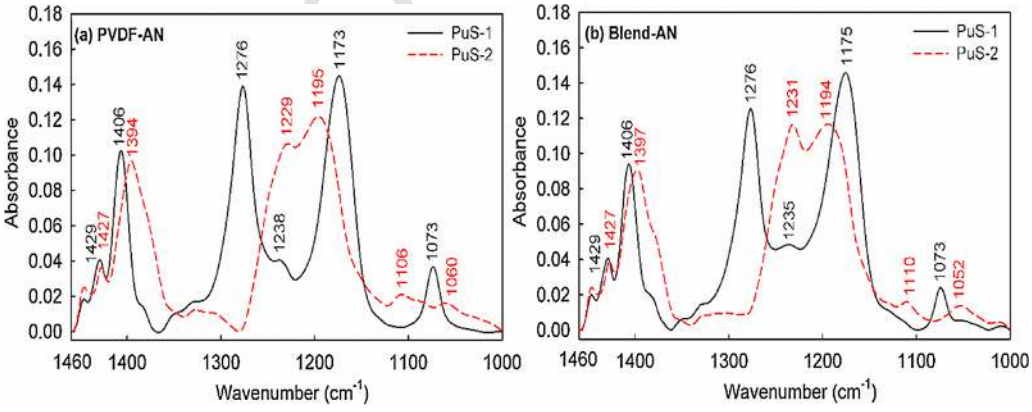

Fig. 4. FTIR-TS: Extracted pure-component spectra (PuS-1 and 2) using FA of (a) PVDF and (b) PVDF/HBP blend (90/10). Annealed (AN, 130 °C) samples were used in this study.

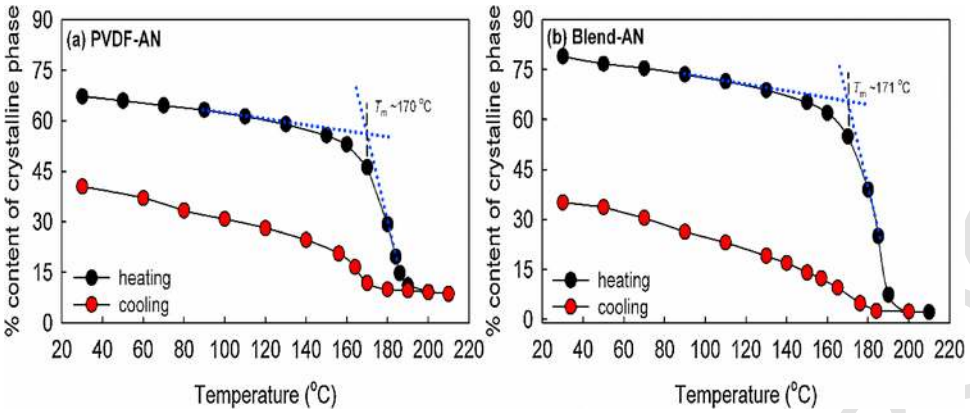

Fig. 5. FTIR-TS: Percentage content of β-crystalline phase calculated using FA of (a) PVDF and (b) PVDF/HBP blend (90/10). Annealed (AN, 130 °C) samples were used in this study.

AN and blend-AN samples at 30 °C during the heating cycle was calculated to be 67% (59% for AC case) and 79% (67% for AC case), respectively. The ordered ferroelectric phase is transformed to disordered amorphous phase in the melting range (~170 °C) during heating cycle for both the samples which indicate the loss of dipole orientation. β-phase content in PVDF-AN and blend-AN were reduced to 40% (27% for AC case) and 35% (25% for AC case), respectively, when cooled to 30 °C from melt, though not drastically as in the case of AC samples. For PVDF-AN, the β-crystalline content increased by around 8% and 13% during heating and cooling temperatures at 30 °C, respectively, compared to PVDF-AC sample used in the present study and also higher than that observed in the PVDF/TrFE (72/28)-AN case [28]. Addition of HBP in PVDF further increased the β-crystalline content by ~12% at 30 °C during heating cycle. This comparative data is an indication that the PVDF-AN and Blend-AN samples could serve as an alternative to PVDF/TrFE in NvRAM applications. Thus, the annealing process influence an increase in the number of dipoles oriented normal to polymer chain axis and also in the conversion of some of the amorphous phase into ferroelectric β-crystalline phase. Additionally, the reversible phase transition in PVDF-TrFE between low-temperature ↔ high-temperature crystalline phases attributed to its unique Curie transition temperature [30,31] is not observed in the present study using PVDF, which means that higher service temperature range could be used for PVDF compared to PVDF-TrFE.

3.2. Phase transition studies using FTIR-GIRAS

The phase transition behavior of PVDF and PVDF/HBP (90/10) blend AC and AN samples studied using FTIR-GIRAS technique under a heating–cooling (30→210→30 °C) cycle is shown in Fig. 6. The data obtained is similar to that obtained using FTIR-TS studies except the fact that FTIR-GIRAS is sensitive to dipole and chain orientation bands. A_1 band ($\vec{\mu}\|\vec{b}$) associated with the ferroelectric crystalline phase appearing at 1274 cm^{-1} (PVDF) and 1272 cm^{-1} (blend) is sensitively detected by FTIR-GIRAS technique and its absorption intensity is enhanced exclusively, whereas the B_1 band corresponding to chain orientation ($\vec{\mu}\|\vec{c}$) at 1413 cm^{-1} for both PVDF and blend samples showed reduced absorption intensity compared to that observed under FTIR-TS mode. The B_2 absorption intensity band (B_2, $\vec{\mu}\|\vec{a}$) at 1199 cm^{-1} for both PVDF and the blend samples associated with $\nu_{as}CF_2$ is reduced remarkably for both the samples unlike AC and AN of PVDF and its blend samples measured using FTIR-TS mode.

3.2.1. FTIR-GIRAS: factor analysis of AC samples

Spectral features of high-temperature and low-temperature phases during a heating-cooling (30→210→30 °C) cycle were studied using FA of the 24 and 19 reflection absorption spectra recorded for PVDF-AC and blend-AC samples, respectively. Frequency range of 1500–1050 having 206 data points for both PVDF-AC and blend-AC sam-

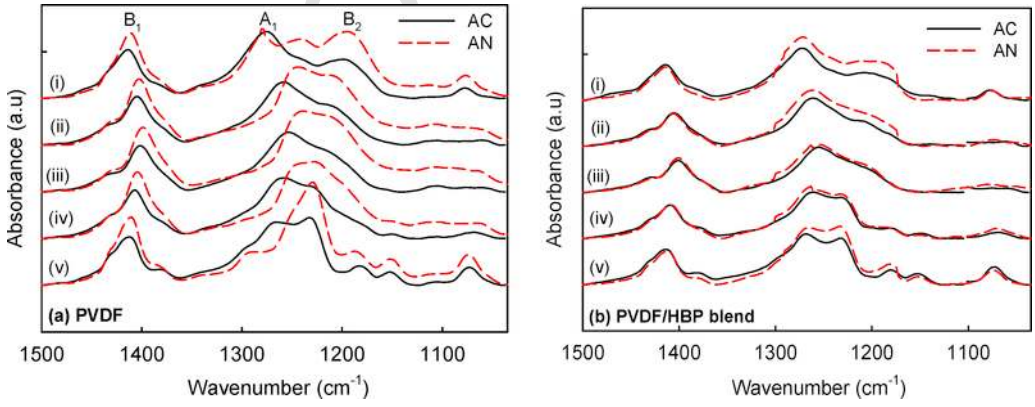

Fig. 6. FTIR-GIRAS: Temperature induced changes in (a) PVDF and (b) PVDF/HBP (90/10) samples (AC and AN) as a function of heating(H)–cooling(C) sequence in the order of (i) 30H, (ii) 140H, (iii) 210H, (iv) 125C and (v) 30C.

ples were considered during FA to extract the pure component spectra. From the FA data given in Table 2, the number of factors for both the samples were determined from the $(IND)_k$ value and were found to be 7 and 4 for PVDF-AC and blend-AC, respectively. Eigenspectra and product spectrum of the first eigen spectrum and the second eigen spectrum are represented in Fig. S3 for both the samples.

The bands at 1211 and 1278 cm^{-1} were employed as minima and maxima, respectively in the product spectrum for PVDF-AC sample (Fig. S3) and the 1209 cm^{-1} minima and 1274 cm^{-1} maxima for blend-AC sample were chosen for obtaining the pure-component spectra using FA. Though, the extracted pure-component spectra obtained as a function of annealed samples reported by our group [27] by GIRAS is not conclusive like the literature reported in Ref. [28], the heating-cooling studies by GIRAS is more effective in extracting the pure-component spectra as depicted in Fig. 7. PuS-1 for both the samples represents the ferroelectric low-temperature all-*trans* phase while the PuS-2 represents the high-temperature amorphous phase. Crystalline bands in PuS-1 of PVDF-AC sample are identified at 1378, 1274, 1232, 1184, 1155 and 1074 cm^{-1} whereas for blend-AC sample, the crystalline bands are shifted to lower wavenumber in comparison to that of PVDF-AC sample. The bands at 1274 and 1155 cm^{-1} for PVDF-AC and 1270 and 1151 cm^{-1} for blend-AC samples are non-overlapping with the amorphous phase bands. The bands at 1274 (PVDF) and 1270 cm^{-1} (blend) are considered as ferroelectric crystalline bands and could be used for measuring the sample crystallinity. Except the bands at 1218, 1105 and 1257, 1214 cm^{-1} for PVDF-AC sample and blend-AC samples respectively, all other bands in PuS-2 are overlapping with the crystalline bands of PuS-1. Hence, the non-overlapping bands (1218 for PVDF-AC and 1257, 1214 cm^{-1} for blend-AC) are considered as amorphous phase bands [28,31].

The quantitative estimation of ferroelectric crystalline phase content using FA for PVDF-AC and blend-AC samples from heating-cooling cycle measured using GIRAS is shown in Fig. 8. The ferroelectric content of blend-AC sample at 30 °C during heating was found to be 74%, which is higher than that of PVDF-AC (72%) and P(VDF/TrFE)(72/28)-AN [28] samples. The ferroelectric content after melting at 210 °C for both PVDF-AC and blend-AC samples were found to be 13% and 51%, respectively. The ferroelectric contents for PVDF-AC and blend-AC samples after cooling to 30 °C from melt were found to be 59% and 80%, respectively. The AC sample exhibits a reversible crystalline phase transition with increased ferroelectric crystalline content in the case of blend sample due to the "non-isothermal annealing effect" [8]. The reasons for enhanced ferroelectric content in blend sample is owed to the (i) presence of HBP in the blend mixture and the existence of H-bonding between the carbonyl and/or hydroxyl groups of HBP and $–CH_2$ or $–CF_2$ of PVDF in the blend [40–42], (ii) presence of HBP in nanoscale (2–15 nm) thereby acting as an nanoparticle in the blend mixture [43–45], and/or (iii) the formation of more extended all-trans fractions during cold-crystallization by interrupting the chain mobility or the presence of HBP in the blend nucleating β-crystals, perhaps epitaxially on their

Table 2
FTIR-GIRAS: FA data of PVDF and PVDF/HBP (90/10) AC and AN samples subjected to heating–cooling (30→210→30 °C) cycle.

Components	PVDF-AC		PVDF/HBP-AC		PVDF-AN		PVDF/HBP-AN	
	Eigen value	IND × 10^4	Eigen value	IND × 10^4	Eigen value	IND × 10^4	Eigen value	IND × 10^4
1.	28.2381	**0.1355**	18.5236	**0.3498**	22.2253	**0.2404**	24.0991	**0.2086**
2.	0.4345	**0.0973**	0.3056	**0.2416**	0.4732	**0.1684**	0.4826	**0.1581**
3.	0.3040	**0.0286**	0.1554	**0.0845**	0.2793	**0.0516**	0.3912	**0.0449**
4.	0.0116	**0.0224**	0.0073	**0.0722**	0.0128	**0.0381**	0.0139	**0.0352**
5.	0.0036	**0.0207**	0.0019	0.0750	0.0034	**0.0348**	0.0025	0.0358
6.	0.0017	**0.0205**	0.0015	0.0783	0.0025	**0.0306**	0.0020	0.0366
7.	0.0015	**0.0201**	0.0013	0.0818	0.0011	**0.0293**	0.0017	0.0376
8.	0.0009	0.0205	0.0008	0.0884	0.0005	0.0302	0.0011	0.0397
9.	0.0009	0.0204	0.0006	0.0981	0.0004	0.0314	0.0010	0.0420
10–17	Not shown here							
18.	0.0001	0.0404	0.0000	4.0034	0.0000	0.1391	0.0002	0.1342
19.	0.0000	0.0553	0.0000	–	0.0000	0.2009	0.0002	0.2296
20.	0.0000	0.0829			0.0000	0.3224	0.0001	0.5496
21.	0.0000	0.1404			0.0000	0.7058	0.0000	4.3646
22.	0.0000	0.3251			0.0000	2.6991	0.0000	–
23.	0.0000	2.0716			0.0000	–		
24.	0.0000	–						

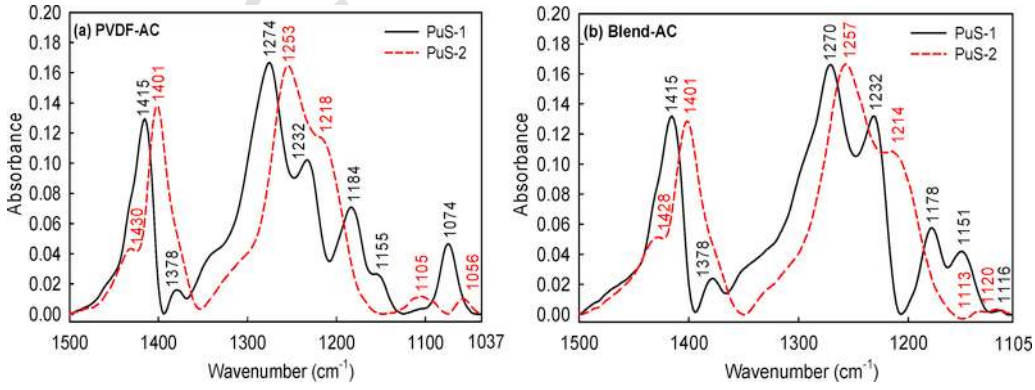

Fig. 7. FTIR-GIRAS: Extracted pure-component spectra (PuS-1 and 2) using FA of (a) PVDF and (b) PVDF/HBP blend (90/10). As-cast (AC) samples were used in this study.

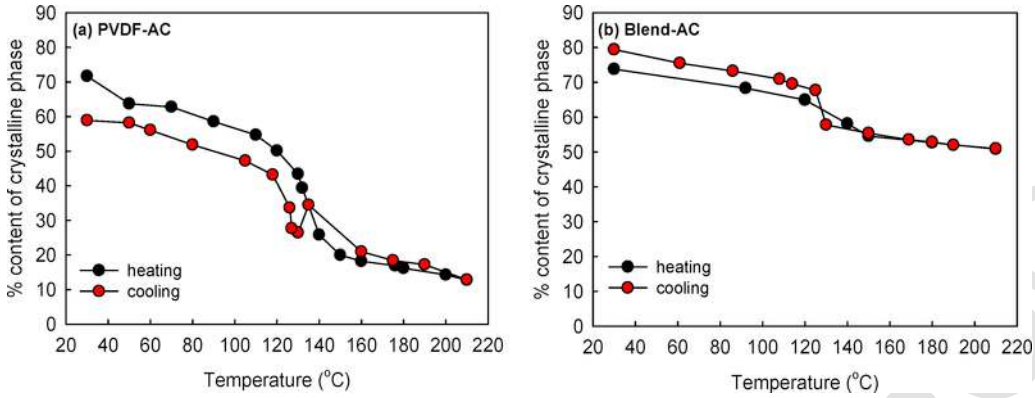

Fig. 8. FTIR-GIRAS: Percentage content of β-crystalline phase calculated using FA of (a) PVDF and (b) PVDF/HBP blend (90/10). As-cast (AC) samples were used in this study.

surfaces [44,46]. The reversible phase transition between the low-temperature and high-temperature phase detected in the range of 130–150 °C for both the samples implies the existence of polarization at higher temperature range than that observed from other earlier studies using P(VDF/TrFE) (72/28) sample [28].

3.2.2. FTIR-GIRAS: factor analysis of AN samples

In order to calculate the ferroelectric crystalline phase content and to determine the working temperature range of ultrathin film based devices for electronic applications, 23 and 22 spectra of PVDF-AN and PVDF/HBP blend (90/10)-AN samples, respectively were subjected to a heating-cooling cycle (30→210→30 °C). Frequency range of 1500–1000 cm^{-1} containing 260 data points for both the samples were considered for extracting the pure component phases using FA. Table 2 shows the FA data of both the samples subjected to heating–cooling cycle. The number of eigenspectra (Fig. S4) can be determined from the number of factors from $(IND)_k$ value given in Table 2 and were found to be 7 and 4 for PVDF-AN and blend-AN samples, respectively. The product spectrum obtained by the product of the 1st and 2nd eigenspectra is depicted in Fig. S4 for both the samples. Minima and maxima were observed at 1276 and 1228 cm^{-1}, respectively for PVDF-AN sample, and the minima and maxima observed at 1251 and 1274 cm^{-1}, respectively for blend-AN sample were employed for obtaining the pure-component spectra using FA. The extracted pure-component spectra designated as PuS-1 and PuS-2 (Fig. 9) represent the low-temperature and high-temperature phases, respectively. The crystalline bands (in PuS-1) of PVDF-AN sample appear at 1278, 1199, 1083 and 1054 cm^{-1}, and in the case of blend-AN sample, the crystalline bands appear at 1270, 1232, 1182, 1153 and 1074 cm^{-1}.

Since, the 1278 cm^{-1} crystalline band is overlapped with the 1297 cm^{-1} band of high-temperature phase spectrum, it is not considered for measuring sample crystallinity in the case of PVDF-AN sample. An increase in the chain orientation absorption band intensity (B_1) may have resulted in some interference of B_1 sensitive band over A_1 and B_2 sensitive bands, and since FA can be used for binary mixtures containing only two factors, the presence of a third component probably sensitive to chain orientation may have resulted in the partially overlapped crystalline and amorphous bands [28] as observed in annealed samples by GIRAS. All the crystalline bands except 1232 and 1074 cm^{-1} of PuS-1 of PVDF-AN sample are non-overlapping bands with the amorphous bands of PuS-2. Though the crystalline bands at 1270, 1182 and 1153 cm^{-1} are non-overlapping bands, the 1270 cm^{-1} is considered for measuring the ferroelectric crystallinity of the sample whereas, the non-overlapping bands at 1228 and 1149 cm^{-1} are considered as amorphous phases as shown in Fig. 9(a) for PVDF-AN sample. In the case of blend-AN sample, the bands obtained for PuS-1 are 1380, 1270, 1232, 1182, 1153 and 1074 cm^{-1} as observed from Fig. 9(b). The non-overlapping bands at 1270, 1182 and 1153 cm^{-1} are regarded as low-temperature phases while the band at 1255 cm^{-1} is considered as high-temperature amorphous phase since it is not overlapping with any of the low-temperature bands [28].

The quantitative variation in ferroelectric phase as a function of phase transition temperature is shown in Fig. 10 for PVDF-AN and blend-AN samples. The ferroelectric content of blend-AN at 30 °C

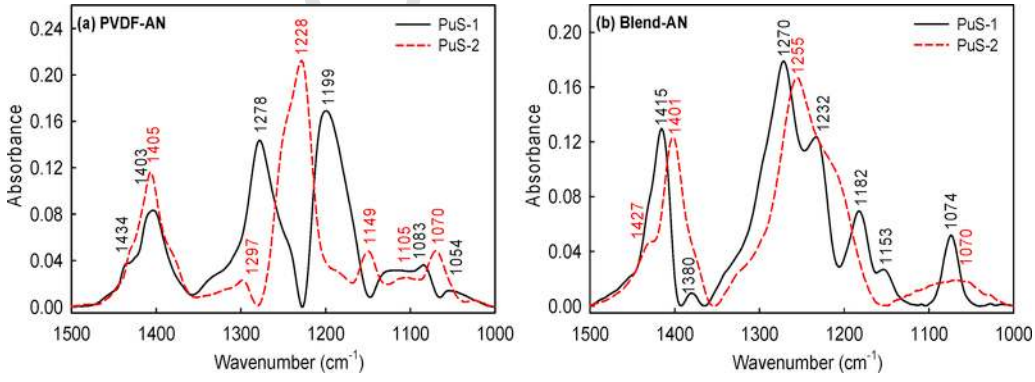

Fig. 9. FTIR-GIRAS: Extracted pure-component spectra (PuS-1 and 2) using FA of (a) PVDF and (b) PVDF/HBP blend (90/10). Annealed (AN, 130 °C) samples were used in this study.

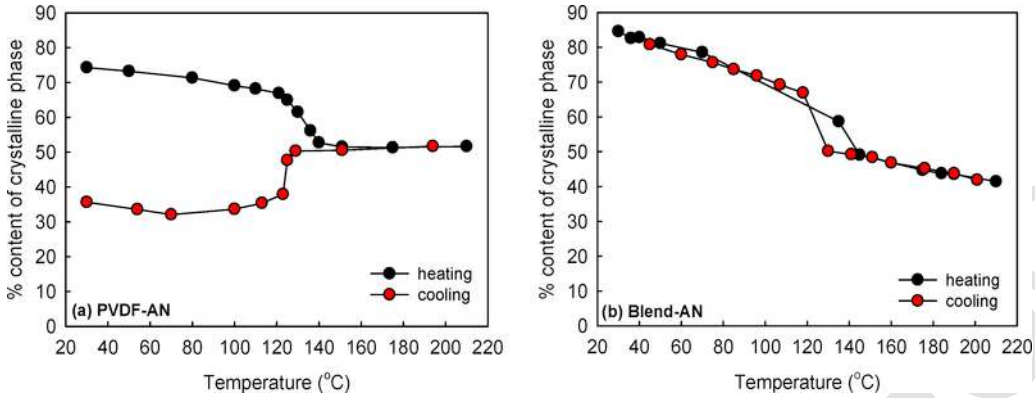

Fig. 10. FTIR-GIRAS: Percentage content of β-crystalline phase calculated using FA of (a) PVDF and (b) PVDF/HBP blend (90/10). Annealed (AN, 130 °C) samples were used in this study.

during heating is higher than that of blend-AC and PVDF-AN by GIRAS and computed to be 85%, which is higher than that of AN-P(VDF/TrFE) (72/28) [28]. In our previous study, the spin-coated P(VDF-TrFE)(72/28) AN sample exhibited an irreversible phase transition occurring at around 120 and 115 °C during heating and cooling, respectively. The crystalline phase that initially formed due to the spin-coating action was destroyed at melt state resulting in reduced ferroelectric crystalline phase content when cooled to room temperature from melt [30]. However, in the present study, the blend-AN sample exhibits a reversible phase transition between the low-temperature and high-temperature phases occurring at near 135 and 120 °C during heating and cooling, respectively. The higher amount of β-phase and the unique reversible hysteresis loop between ordered and disordered phases observed even after cooling from melt exhibited by blend-AN sample makes it suitable for use in the fabrication of electronic devices such as non-volatile memory, sensors, etc. with higher operating temperature range. Such reversible crystalline phase behavior is not observed in the case of PVDF-AN sample, which implies the importance of the role played by HBP as a suitable blend component for improving the ferroelectric phase in PVDF.

4. Conclusion

As-cast (AC, at 30 °C) and annealed (AN, at 130 °C) samples of PVDF and PVDF/HBP blend (90/10) ultrathin films were studied for their changes in β-crystalline behavior under heating-cooling (30→210(>T_m)→30 °C) cycle measured using in situ FTIR-TS and FTIR-GIRAS modes. Pure high-temperature and low-temperature spectra as well as quantification of the ferroelectric crystalline content were carried out using FA of the samples used in this study. From the FA of FTIR-TS data, AN samples exhibited higher ferroelectric content in comparison to that of AC samples. Compared to FTIR-TS technique, FTIR-GIRAS is more sensitive to dipole and chain-orientation changes. Interestingly, from the FA of FTIR-GIRAS data, blend-AC sample was found to exhibit a reversible crystalline phase transition with increased ferroelectric crystalline content than PVDF-AC sample aided by the "non-isothermal annealing effect." The reason for enhanced ferroelectric content in the blend sample is owed to the (i) the existence of H-bonding between the carbonyl and/or hydroxyl groups of HBP and $-CH_2$ or $-CF_2$ of PVDF in the blend and (ii) the presence of HBP in nanoscale (2–15 nm) thereby acting as an nanoparticle in the blend mixture. The reversible phase transition between the low-temperature and high-temperature phase detected in the range of 130–150 °C for both the samples implies the existence of polarization at higher temperature range than that observed from other earlier studies using P(VDF/TrFE) (72/28). The higher amount of β-phase and the unique reversible hysteresis loop between ordered and disordered phases observed even after cooling from melt exhibited by blend-AN sample makes it suitable for use in the fabrication of electronic devices such as non-volatile memory, sensors, etc. with higher operating temperature range. Such reversible crystalline phase behavior is not observed in the case of PVDF-AN sample.

Among two different FTIR modes used in this study, FTIR-GIRAS data is more preferred than using FTIR-TS data for the following reasons:

FTIR-TS using KBr as the measurement substrate is not preferred due to the fact that the substrates used for memory devices (Gold or ITO coated glass slides) are not IR transparent. On the other hand, the substrate used for measuring FTIR-GIRAS (Gold or ITO coated glass slides) is similar to that used in the fabrication of electronic devices and hence the data obtained from GIRAS is more reliable than that obtained from TS technique.

Due to the inherent measuring parameters like variable angle of incidence (ca. 80–88° from the normal to the surface) and polarization of the incident i.r. beam (into *s*- and *p*- polarization) upon reflectance from the surface, GIRAS data is more sensitive to chain and dipole orientations, and can be effectively used in identifying the best sample conditions suitable for device fabrication.

Overall, the data extracted from this study were useful in identifying the best possible sample preparation condition (AN) that exhibit maximum β-crystalline content along with favorable chain and dipole orientations ((PVDF/HBP) blend (90/10) sample spin-cast on ITO) suitable for use in NvRAM devices.

Acknowledgement

This work was supported by the Industrial Strategic Technology Development Program (Grant no. 10047976) funded by the Ministry of Trade, Industry & Energy (MOTIE, KOREA).

Appendix A. Supplementary data

Supplementary material related to this article can be found, in the online version, at https://doi.org/10.1016/j.vibspec.2017.12.003.

References

[1] C. Li, W.D. Fan, B. Lei, D.H. Zhang, S. Han, T. Tang, Appl. Phys. Lett. 84 (2004) 1949–1951.
[2] P. Heremans, G.H. Gelinck, R. Muller, K.J. Baeg, D.Y. Kim, Y.Y. Noh, Chem. Mater. 23 (2011) 341–358.

[3] L. Zhang, Y. Li, J. Shi, G. Shi, S. Cao, Mater. Chem. Phys. 142 (2013) 626–632.
[4] S.G. Hahm, Y.G. Ko, W. Kwon, M. Ree, Curr. Opin. Chem. Eng. 2 (2013) 79–87.
[5] S. Hong, O. Auciello, D. Wouters, Emerging Non-Volatile Memories, 1st ed., Springer, New York, 2014.
[6] H.G. Kassa, L. Nougaret, R. Cai, A. Marrani, B. Nysten, Z. Hu, A.M. Jonas, Macromolecules 47 (2014) 4711–4717.
[7] Q.D. Ling, D.J. Liaw, E.Y.H. Teo, C. Zhu, D.S.H. Chan, E.T. Kang, K.G. Neoh, Polymer 48 (2007) 5182–5201.
[8] C.C. Choi, A.A. Prabu, Y.M. Kim, S. Yoon, K.J. Kim, C. Park, Appl. Phys. Lett. 93 (2008) 182902.
[9] D. Kim, D.Y. Khang, Polymer 55 (2014) 2491–2495.
[10] T. Furukawa, Ferroelectrics 57 (1983) 63–72.
[11] S.S. Guo, W.P. Li, C.L. Sun, D.H. Wang, X.Z. Zhao, S.T. Lau, H.L.W. Chan, Mater. Chem. Phys. 81 (2003) 166–173.
[12] S. Ducharme, T.J. Reece, C.M. Othon, R.K. Rannow, IEEE Trans. Device Mater. Reliab. 5 (2005) 720–735.
[13] M.P. Silva, V. Sencadas, G. Botelho, A.V. Machado, A.G. Rolo, J.G. Rocha, S.L. Mendez, Mater. Chem. Phys. 122 (2010) 87–92.
[14] M. Mai, S. Ke, P. Lin, X. Zeng, J. Nanomater 2015 (2015) 1–14.
[15] S. Yoon, A.A. Prabu, K.J. Kim, C. Park, Macromol. Rapid Commun. 29 (2008) 1316–1321.
[16] J. Yang, S. Pruvost, S. Livi, J.D. Rumeau, Understanding of versatile and tunable nanostructuration of ionic liquids on fluorinated copolymer, Macromolecules 48 (2015) 4581–4590.
[17] D. Okada, H. Kaneko, K. Kato, S. Furumi, M. Takeguchi, Y. Yamamoto, Macromolecules 48 (2015) 2570–2575.
[18] Y. Zhu, C. Li, Bing Na, R. Lv, B. Chen, J. Zhu, Mater. Chem. Phys. 144 (2014) 194–198.
[19] C.W. Tang, B. Li, L. Sun, B. Lively, W.H. Zhong, Eur. Polym. J. 48 (2012) 1062–1072.
[20] D. Mandal, K.J. Kim, J.S. Lee, Langmuir 28 (2012) 10310–10317.
[21] N. Jia, Q. Xing, G. Xia, J. Sun, R. Song, W. Huang, Mater. Lett. 139 (2015) 212–215.
[22] R. Neppalli, S. Wanjale, M. Birajdar, V. Causin, Eur. Polym. J. 49 (2013) 90–99.
[23] F.C. Chiu, Mater. Chem. Phys. 143 (2014) 681–692.
[24] C.X. Feng, J. Duan, J.H. Yang, T. Huang, N. Zhang, Y. Wang, X.T. Zheng, Z.W. Zhou, Eur. Polym. J. 68 (2015) 175–189.
[25] K. Ke, P. Potschke, D. Jehnichen, D. Fischer, B. Voit, Polymer 55 (2014) 611–619.
[26] H. Luo, Y. Huang, D. Wang, Polymer 54 (2013) 4710–4718.
[27] D.M. Dhevi, A.A. Prabu, M. Pathak, Polymer 55 (2014) 886–895.
[28] A.A. Prabu, J.S. Lee, K.J. Kim, H.S. Lee, Vib. Spectrosc. 41 (2006) 1–13.
[29] L. Yang, X. Li, E. Allahyarov, P.L. Taylor, Q.M. Zhang, L. Zhu, Polymer 54 (2013) 1709–1728.
[30] P. Sathiyanathan, D.M. Dhevi, A.A. Prabu, K.J. Kim, Adv. Mater. Res. 584 (2012) 201–204.
[31] A.A. Prabu, K.J. Kim, C. Park, Vib. Spectrosc. 49 (2009) 101–109.
[32] D.M. Dhevi, A.A. Prabu, H. Kim, M. Pathak, J. Polym. Res. 21 (2014) 1–9.
[33] S. Ramasundaram, S. Yoon, K.J. Kim, J.S. Lee, Macromol. Chem. Phys. 209 (2008) 2516–2526.
[34] M. Kobayashi, K. Tashiro, H. Tadokoro, Macromolecules 8 (1975) 158–171.
[35] K. Tashiro, Y. Itoh, M. Kobayashi, H. Tadokoro, Macromolecules 18 (1985) 2600–2606.
[36] K.J. Kim, N.M. Reynolds, S.L. Hsu, Macromolecules 22 (1989) 4395–4401.
[37] K.J. Kim, N.M. Reynolds, S.L. Hsu, J. Polym. Sci. Part B: Polym. Phys. 31 (1993) 1555–1566.
[38] T. Furukawa, Phase Transit. 18 (1989) 143–211.
[39] K. Tashiro, K. Takano, M. Kobayashi, Y. Chatani, H. Tadokoro, Ferroelectrics 57 (1984) 297–326.
[40] K.J. Kim, Y.J. Cho, Y.H. Kim, Vib. Spectrosc. 9 (1995) 147–159.
[41] M. Benz, W.B. Euler, O.J. Gregory, Macromolecules 35 (2002) 2682–2688.
[42] X. He, K. Yao, Appl. Phys. Lett. 89 (2006) 112909.
[43] C. Leonard, J.L. Halary, L. Monnerie, Macromolecules 21 (1988) 2988–2994.
[44] J. Buckley, P. Cebe, D. Cherdack, J. Crawford, B.S. Ince, M. Jenkins, Polymer 47 (2006) 2411–2422.
[45] D. Yan, C. Gao, H. Frey, Hyperbranched Polymers Synthesis, Properties, and Applications, J. Wiley & Sons, Inc/, Hoboken, New Jersey, 2010.
[46] L. Priya, J.P. Jog, J. Polym. Sci. Part B: Polym. Phys. 41 (2003) 31–38.